LA-UR- 98-300

Approved for public release; distribution is unlimited.

Title: PROGRESS IN SMOOTH PARTICLE HYDRODYNAMICS

CONF- 9711159--

Author(s): C. Wingate
G. Dilts
L. Crotzer
C. Knapp
D. Mandell

Submitted to: Shock Physics Conference
Oxford, England
November 1997

Los Alamos
NATIONAL LABORATORY

DISCLAIMER

Progress in Smooth Particle Hydrodynamics

C. A. Wingate, G. A. Dilts, D. A. Mandell, L. A. Crotzer and C. E. Knapp

Los Alamos National Laboratory, MS D413, Los Alamos, NM 87545

ABSTRACT

Smooth Particle Hydrodynamics (SPH) is a meshless, Lagrangian numerical method for hydrodynamics calculations where calculational elements are fuzzy particles which move according to the hydrodynamic equations of motion. Each particle carries local values of density, temperature, pressure and other hydrodynamic parameters. A major advantage of SPH is that it is meshless, thus large deformation calculations can be easily done with no connectivity complications. Interface positions are known and there are no problems with advecting quantities through a mesh that typical Eulerian codes have. These underlying SPH features make fracture physics easy and natural and in fact, much of the applications work revolves around simulating fracture. Debris particles from impacts can be easily transported across large voids with SPH.

While SPH has considerable promise, there are some problems inherent in the technique that have so far limited its usefulness. The most serious problem is the well known instability in tension leading to particle clumping and numerical fracture. Another problem is that the SPH interpolation is only correct when particles are uniformly spaced a half particle apart leading to incorrect strain rates, accelerations and other quantities for general particle distributions. SPH calculations are also sensitive to particle locations. The standard artificial viscosity treatment in SPH leads to spurious viscosity in shear flows.

This paper will demonstrate solutions for these problems that we and others have been developing. The most promising is to replace the SPH interpolant with the moving least squares (MLS) interpolant invented by Lancaster and Salkauskas in 1981. SPH and MLS are closely related with MLS being essentially SPH with corrected particle volumes. When formulated correctly, MLS is conservative, stable in both compression and tension, does not have the SPH boundary problems and is not sensitive to particle placement. The other approach to solving SPH problems, pioneered by Randles and Libersky, is to use a different SPH equation and to renormalize the kernel gradient sums.

Finally we present results using the SPH statistical fracture model (SPHSFM). It has been applied to a series of ball on plate impacts performed by Grady and Kipp. A description of the model and comparison with the experiments will be given.

PHILOSOPHY OF SPH

SPH is a gridless Lagrangian hydrodynamic computational technique. With some care, it can be written in a fully conservative form. The form of the SPH equations is extremely simple, even in 3 dimensions. These characteristics, together with the physical "feeling" for the problem that is embodied in a fully Lagrangian code makes SPH an attractive approach for problems with complicated geometry, large void areas, fracture, or chaotic flow fields.

SPH was first derived by Lucy (1977) as a Monte-Carlo approach to solving the hydrodynamic time evolution equations. Subsequently, Monaghan and co-workers (Monaghan 1982, 1985, 1988, Gingold and Monaghan 1977, 1982) reformulated the derivation in terms of an interpolation theory, which was shown to better estimate the error scaling of the technique. According to the interpolation derivation, each SPH "particle" represents a mathematical interpolation point at which the fluid properties are known. The complete solution is obtained at all points in space by application of an interpolation function. This function is required to be continuous and differentiable. Gradients that appear in the flow equations are obtained via analytic differentiation of the smooth, interpolated functions. Monaghan showed that other well known techniques, such as PIC, finite element, and finite volume methods could also be derived in this way through appropriate choice of interpolation technique. SPH is distinguished by the simplicity of its approach: interpolation is done by summing over "kernels" associated with each particle. Each kernel is a spherically symmetric function centered at the particle location and generally resembling a Gaussian in shape. The order of accuracy of the interpolation (and thus of the difference equations) is determined by the smoothness of the kernel. The kernel is required to approach a delta function in the limit of small extent. The interpolation is accomplished by summing each equation or variable at any location over nearby known values at particle locations, each weighted by its own kernel weighting function. Each kernel function is required to integrate over all space to exactly unity, thus normalizing the interpolation sums. By appropriately modifying the normalization condition, the same code can easily switch between 1D, 2D, 3D, spherical or cylindrical geometric configurations. This feature allows code development in 1D or 2D, with confidence that the same coding will work for all cases if implemented carefully. An excellent review of SPH can be found in Benz (1989 and 1990).

The original SPH code at Los Alamos is SPHC, which was written by Bob Stellingwerf when he was at MRC (Stellingwerf 1989a, 1989b, 1990a, 1990b, 1992 and Stellingwerf and Peterkin 1990). The current production code is SPHINX, which is a parallel version with a more convenient user interface and an integrated X-Windows graphic runtime display. SPHINX is the production code used for high resolution 2D and 3D modeling and is currently being developed by several people at Los Alamos.

FLUID EQUATIONS

SPHINX solves the general fluid dynamics equations. The first of these is the continuity equation

$$\frac{d\rho}{dt} + \rho \frac{\partial}{\partial x^\alpha} U^\alpha = 0 \tag{1}$$

where ρ is the material density and U is the material velocity. We use Greek superscripts to indicate coordinate directions with implied summation on repeated indices. Roman subscripts will be used to label particles. Summation is not implied on repeated subscripts (the summation sign must appear directly).

The second equation is the momentum equation

$$\frac{d}{dt} U^\alpha = \frac{1}{\rho} \frac{\partial}{\partial x^\beta} \sigma^{\alpha\beta} \tag{2}$$

where $\sigma^{\alpha\beta}$ is the stress tensor. This is divided into an isotropic part which is the pressure P and a traceless deviatoric stress tensor $S^{\alpha\beta}$ given by:

$$\sigma^{\alpha\beta} = -P\delta^{\alpha\beta} + S^{\alpha\beta}. \tag{3}$$

The final equation is the energy equation:

$$\frac{de}{dt} = \frac{1}{\rho}\sigma^{\alpha\beta}\dot{\varepsilon}^{\alpha\beta}, \tag{4}$$

where e is the specific internal energy and $\dot{\varepsilon}$ is the strain rate tensor given by

$$\dot{\varepsilon}^{\alpha\beta} = \frac{1}{2}\left(\frac{\partial}{\partial x^{\beta}}U^{\alpha} + \frac{\partial}{\partial x^{\alpha}}U^{\beta}\right). \tag{5}$$

Using the definition of the stress tensor (equation 3) and given that the trace of the strain rate tensor is the divergence of the velocity, the energy equation can be rewritten (in perhaps the more familiar form) as:

$$\frac{de}{dt} = -\frac{P}{\rho}\frac{\partial}{\partial x^{\alpha}}U^{\alpha} + \frac{1}{\rho}S^{\alpha\beta}\dot{\varepsilon}^{\alpha\beta}. \tag{6}$$

The procedure for converting the analytic equations into interpolated SPH equations is described in many places, for example see Monaghan (1988) or Benz (1989). Here we list the results. The continuity equation is sometimes solved in integral form as:

$$\rho_i = \sum_j m_j W_{ij} \tag{7}$$

where m_j is the mass of particle j and W_{ij} is the smoothing kernel. The kernel could be written as $W_{ij}(|r_i - r_j|, h)$ to indicate its dependence on the distance between particles i and j and its dependence on the smoothing length h. For simplicity, however, we will write it simply as W_{ij}. The smoothing length is a measure of the width of the kernel, and may vary from particle to particle. The kernel in SPINX used in these calculations is a cubic B-spline designated as W4 in Gingold and Monaghan (1982).

The momentum equation in the SPH approximation becomes:

$$\frac{d}{dt}U_i^{\alpha} = \sum_j m_j\left(\frac{\sigma_i^{\alpha\beta}}{\rho_i^2} + \frac{\sigma_j^{\alpha\beta}}{\rho_j^2}\right)\frac{\partial W_{ij}}{\partial x^{\beta}}. \tag{8}$$

If this equation is multiplied by m_i we see that the time derivative of the momentum is exactly symmetric in i and j thus ensuring exact conservation of both linear and angular momentum.

The energy equation in the SPH approximation is:

$$\frac{de_i}{dt} = \frac{1}{2}\sum_j m_j(U_j^{\alpha} - U_i^{\alpha})\left(\frac{\sigma_i^{\alpha\beta}}{\rho_i^2} + \frac{\sigma_j^{\alpha\beta}}{\rho_j^2}\right)\frac{\partial W_{ij}}{\partial x_i^{\beta}}. \tag{9}$$

Multiplying this equation by m_i, summing over i, and using equation 8, we can prove exact energy conservation for the full system of particles. A rearrangement of terms in the energy sum formed

from equation (9) produces the form of the energy equation used in SPHINX, and is also exactly conservative:

$$\frac{de_i}{dt} = \sum_j m_j (U_j^\alpha - U_i^\alpha)\left(\frac{\sigma_i^{\alpha\beta}}{\rho_i^2}\right)\frac{\partial W_{ij}}{\partial x_i^\beta}. \tag{10}$$

To obtain the particle approximation for the strain rate tensor we follow Libersky and Petschek (1990) to get

$$\dot{\varepsilon}_i^{\alpha\beta} = \frac{1}{2}\sum_j \frac{m_j}{\rho_j}\left((U_j^\alpha - U_i^\alpha)\frac{\partial W_{ij}}{\partial x_i^\beta} + (U_j^\beta - U_i^\beta)\frac{\partial W_{ij}}{\partial x_i^\alpha}\right). \tag{11}$$

ELASTIC PERFECTLY PLASTIC STRENGTH MODEL

The strength model installed in SPHINX is a basic Hooke's law model where the stress deviator rate is proportional to the strain rate. This type of model was first used in a smooth particle hydrodynamic code by Libersky and Petschek (1990). The elastic constitutive equation which relates the deviatoric stress rate to the strain rate can be found in various places, and is given by

$$\frac{d}{dt}S^{\alpha\beta} = 2\mu\left(\dot{\varepsilon}^{\alpha\beta} - \frac{1}{3}\delta^{\alpha\beta}\dot{\varepsilon}^{\gamma\gamma}\right) + S^{\alpha\gamma}R^{\beta\gamma} + S^{\gamma\beta}R^{\alpha\gamma} \tag{12}$$

where μ is the shear modulus, and R is the rotation rate tensor defined by

$$R^{\alpha\beta} = \frac{1}{2}\left(\frac{\partial}{\partial x^\beta}U^\alpha - \frac{\partial}{\partial x^\alpha}U^\beta\right). \tag{13}$$

The SPH approximation to the rotation rate tensor is identical to the SPH approximation for the strain rate tensor, equation 11, with the plus sign replaced by a minus sign

$$R_i^{\alpha\beta} = \frac{1}{2}\sum_j \frac{m_j}{\rho_j}\left((U_j^\alpha - U_i^\alpha)\frac{\partial W_{ij}}{\partial x_i^\beta} - (U_j^\beta - U_i^\beta)\frac{\partial W_{ij}}{\partial x_i^\alpha}\right). \tag{14}$$

The von Mises yield criterion is used for plastic flow. This criterion limits the deviatoric stress in the following way. Define a quantity f by

$$f = min\left(\left(\frac{Y_0^2}{3J}\right)^{1/2}, 1\right) \tag{15}$$

where Y_0 is the yield stress and J is the second invariant of the deviatoric stress tensor

$$J = \frac{1}{2}S^{\alpha\beta}S^{\alpha\beta}. \tag{16}$$

The deviatoric stress tensor is then limited by

$$S^{\alpha\beta} = fS^{\alpha\beta}. \tag{17}$$

PHYSICS AND MATERIAL PROPERTIES

A variety of equations of state are available in SPHINX. The most heavily used model is the Grueneissen EOS. In addition, the codes can access the LANL SESAME material property library for all available materials.

Strength models currently implemented are: elastic-perfectly plastic, Bodner-Partom, Johnson-Cook, and Steinberg-Guinan. Each model accesses its own data base of material properties. Implementation details of these models can be found in Libersky and Petschek (1990) and Wingate and Fisher (1992).

Other physics installed in SPHINX include high explosives modeling, fracture (discussed below), and external gravitation. Work is in progress on a composites model.

Numerical techniques in SPHINX include variable smoothing length, arbitrary dimensionality, ghost particle boundary conditions, parallel operation, implicit SPH, and interactive run-time graphics.

OBLIQUE IMPACTS

The calculations of a sphere obliquely impacting a bumper modeled a NASA impact experiment similar to EH1C (Schonberg. et. al., 1988). The sphere was made of 1100 Aluminum with a radius of 0.476 cm, a velocity of 7.0 km/s and a 60 degree angle from the normal. The bumper was 6061-T6 Aluminum with a thickness of 0.16 cm. The calculation was done in 3 dimensions using SPHINX with 113,000 particles. The equation of state used was Grueneissen. The strength model was elastic perfectly plastic with a shear modulus of 265 kbar and a yield strength of 0.345 kbar for the 1100 Al and 2.75 kbar for the 6061-T6 Al. The configuration after 20 microseconds is shown in Figure 1, side projection. Some projectile material scraped from the top of the projectile upon impact has slid along the plate and continued to the left, followed by ejected target material above the plane of impact. The long feature so formed is travelling ballistically to the left - there is no boundary beyond that shown in the figure. Below the target, the projectile material is located at the left edge of the debris cloud, while target material forms the bulk of the rest of the cloud. These results are matched very closely with unpublished experimental results obtained by Andy Piekutowski at UDRI (experiment 4-1439) shown in Figure 2.

FRACTURE

The results of a hydrocode simulation depend on several factors including the particular way its fracture model is implemented. In general, fracture models must be tailored to the type of code, Lagrangian, Eulerian, or smooth particle hydrodynamics (SPH), so that physically realistic cracks result in the context of the code's numerical treatment. But even the same model, implemented into two hydrocodes of the same type but with different coding details, can produce different results.

Statistical fracture models should incorporate a number of features including 1) the introduction of a random distribution of flaws, 2) a differential equation for evolving the local damage variable, 3) formulas for degrading the material strength, modifying the equation of state (EOS), and relax

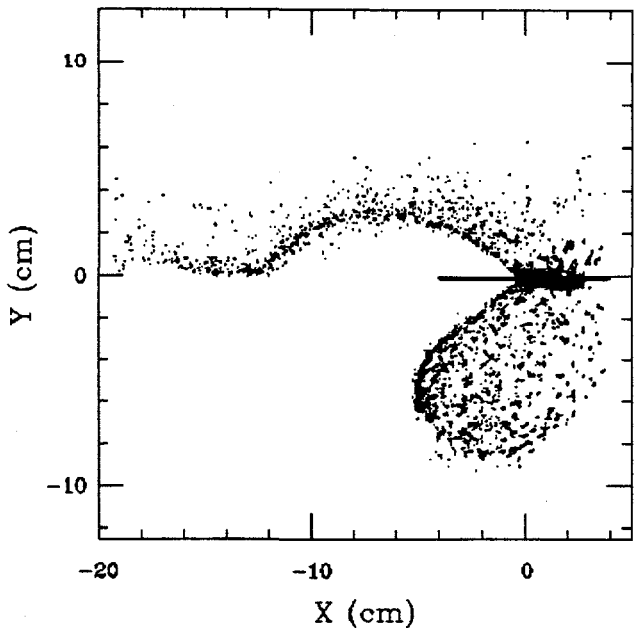

Fig. 1. Oblique impact model, projectile is a sphere entering at an angle of 60 degrees from the normal moving from top right to bottom left. See text for details.

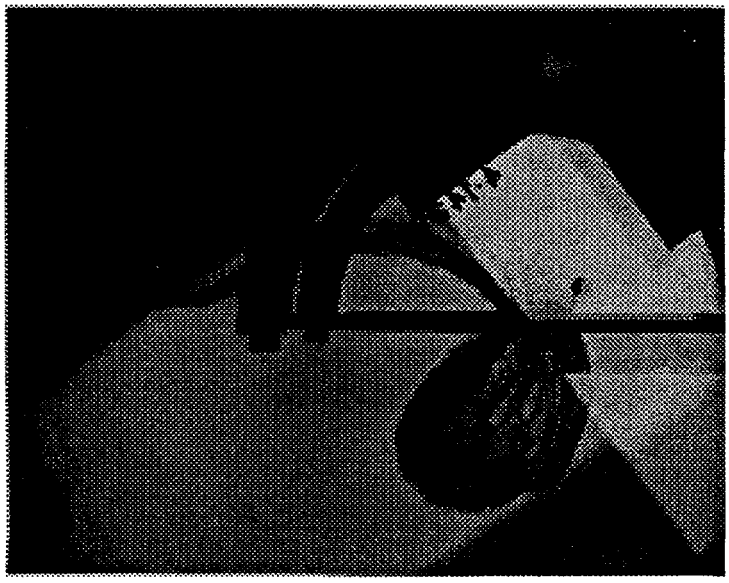

Fig. 2. Experimental data for an experiment very similar to that calculated in Figure 1 (Andy Piekutowski, UDRI).

ing the stress components of the damaged material, and 4) methods for producing and representing cracks in the computational mesh. All of these components are interdependent and must function in mutually compatible ways if the experiments are to be modeled accurately.

The SPH numerical method has certain advantages over other methods for modeling fracture. For example, once the damage is calculated and the material properties degraded, SPH allows for the natural insertion of voids. SPH offers several additional benefits. Unlike conventional Lagrangian techniques, SPH avoids mesh tangling and is therefore much more robust in its treatment of problems with large material distortions. In problems with large void areas, SPH is more computationally efficient than Eulerian codes, and it avoids advection problems, such as numerical diffusion. SPH, however, does have its own set of problems including instabilities in tension (Swegle, et. al., 1995).

To be useful as a design tool, a hydrocode, along with its material strength and fracture models must be able to predict a wide range of experiments. Many fracture models are able to simulate one-dimensional (1D) flyer plate experiments accurately, but are unable to predict multi-dimensional data. Some models are accurate for a restricted set of geometries and boundary and initial conditions, but not for others. Our goal, which we have not yet reached, is to provide a hydrocode-based design tool with a single model for the strength and fracture of brittle materials that will accurately simulate a wide range of experiments and real applications.

SPHINX includes several of a number of models that have been proposed to simulate dynamic brittle fracture (Benz and Asphaug, 1994 and 1995, Randles, et. al., 1995, Randles and Libersky, 1996, Cagnoux, 1985, Glenn, et. al., 1990). We have applied SPHINX with its Cagnoux-Glenn model (Cagnoux, 1985, Glenn et. al., 1990) to simulate the impacts of steel projectiles on glass (Mandell and Wingate, 1995, Mandell, et. al., 1995, Henninger, et al., 1995). The results of the simulations agreed reasonably well with the global data, such as depth of penetration and the measurements of the free surface velocity on the backside of the target, but we were unable to match finer details of the crack patterns. Nor were we able to predict other experiments with the model parameters that were successful in the glass-impact study.

The Fracture Model

SPH statistical fracture modeling is a relatively new innovation. Benz and Asphaug (1994 and 1995) pioneered this field several years ago with the introduction of two models. We began our investigations of statistical fracture with the model described in their more recent work (Benz and Asphaug, 1995), but in the process of implementing and testing the model in SPHINX, we changed it to such an extent that we consider it to be a different model and refer to it as the smooth particle hydrodynamics statistical fracture (SPHSF) model. The most important differences between the SPHSF model and those published by Benz and Asphaug are the ways we seed the flaws and assign the flaw strengths or threshold stress values at which the flaws initiate damage in their local particles. Benz and Asphaug select flaw strengths as uniform intervals on the domain of the Weibull distribution function (Weibull, 1952 and Ashby and Jones, 1988) and assign the flaws to randomly selected particles. Benz and Asphaug continue the process of assigning flaws to particles until every particle contains at least one flaw. In SPHSF, we begin with an empirical parameter that defines the average number of flaws per unit volume. We then calculate the number of flaws in each particle from a Poisson distribution (Crow, et al., 1960) using the particle volume and the average flaw density. We adopted the new approach to avoid having the final distribution of flaws dependent upon the spatial resolution of the problem. (Although to spare computer memory, we typically limit number of flaws in each particle to the ten weakest.) In principle, once the flaws are seeded we could use any statistical distribution for assigning their strengths. However,

we follow the precedent set by Benz and Asphaug and use the Weibull distribution (Weibull, 1952) although we use a slightly different functional form. We define the distribution as

$$P(\sigma) = 1 - \exp\left(-\frac{V}{V_0} n(\sigma)\right) \tag{18}$$

where V is the volume of the sample, and V_0 is the average sample size per flaw so that the total number of flaws in the material is

$$N = V/V_0. \tag{19}$$

The function $n(\sigma)$ in Equation 1 is defined as

$$n(\sigma) = \left(\frac{\sigma - \sigma_u}{\sigma_0}\right)^m \tag{20}$$

where m, σ_u and σ_0 are parameters that characterize intrinsic properties of the material and are independent of the sample volume. The variable σ is a critical stress at which a given flaw begins to accumulate damage to the particle in which it resides. With these definitions, we interpret Equation 1 as follows: in the limit of large N, $NP(\sigma)$ is the number of flaws in a sample of volume V that have critical stresses less than or equal to σ.

Besides using a different functional form for the Weibull distribution, we also differ from Benz and Asphaug in the way we use the distribution. Instead of defining stresses as uniform intervals on the domain, we use a random number generator to select from the full distribution. We show elsewhere (Stellingwerf and Schwalbe, 1995) how this approach reproduces the expected distribution of the weakest flaw in a collection of samples. The form of Equations 1 and 3 is also consistent with the observations that larger samples (those with larger V) are more likely to break.

The remaining aspects of the SPHSFM model are fairly standard. As we mentioned above, each flaw activates damage when the maximum principal stress in the local particle exceeds the flaw's assigned threshold. We define a scalar damage variable D for each particle as the fraction of its volume that is relieved of stress by the growing cracks. SPHINX evolves the damage variable with the ordinary differential equation,

$$\frac{dD}{dt}^{1/3} = n_i \frac{C_g}{R_s} \tag{21}$$

which is very similar to the one that Benz and Asphaug use (Benz and Asphaug, 1995). In the above damage evolution equation, n_i is the number of active flaws for particle i, C_g is the speed at which the crack grows, which we take as a constant equal to 0.4 times the sound speed, and R_s is a characteristic length. We use the cube root of the particle volume for the characteristic length.

Once we compute the damage, we have to couple it back to the material strength and hydrodynamics calculations. The current version of SPHINX allows us to scale the yield stress and/or shear modulus for each particle linearly between a value corresponding to the intact material and a value corresponding to the fully fractured material. In this work, we use a constant shear modulus and let the yield stress decrease linearly to zero as the damage increases from zero to one. Other authors take different approaches. For example, Benz and Asphaug do not modify their calculation of the stress deviators. Instead, they include a factor of $1 - D$ in the equations where

the stress deviators are used. Randles et al. (1995) modify the bulk modulus and the yield strength in tension only by a factor of $1 - D^2$.

Finally, the codes must have a way to let the particles separate and form cracks and material fragments. Again, different researchers use different methods to achieve particle separation. If a particle is fully damaged $D = 1$, Benz and Asphaug exclude that particle from the SPH summations over the neighboring particles. This exclusion effectively disconnects the damaged particle from its neighbors. Other methods have been used to produce crack structures. Randles et al. (1995) disconnect their damaged particles by reducing the smoothing length h. To prevent adverse effects on the time step, they limit the reduction of h to 0.8 of its original value. SPHINX can use either of these two methods. We use the sum exclusion method, but we do so only when the sum of the pressures of the damaged particle and that of its neighbors is negative. This scheme allows damaged particles to resist compression but not tension.

Steel Sphere Fragmentation

Grady and Kipp (1995) conducted extensive experiments of brittle steel spheres impacted into PMMA plates for a number of velocities and plate thicknesses. Two x-ray positions downstream of the plate recorded the sphere fragment patterns. The x-ray was adjusted so that the plate did not appear in the x-ray. SPHINX 3D calculations of two of these experiments, for a 3.38 mm thick plate, were made using the model described above and an elastic-perfectly plastic material strength model. For a sphere velocity of 3.0 km/sec, the sphere remained intact in the experiment. The SPHSF model parameters were adjusted for this case so that the sphere had only a small amount of surface damage. The 4.57 km/sec experiment was then simulated. The data and calculated sphere fragment patterns are shown in Figure 3 (not to scale) for the second x-ray position. The diameter of the experimental debris pattern was 46 mm and the calculated diameter was 42.8 mm. As can be seen from Fig. 3, the calculated pattern has an umbrella shape, whereas the data is planar. Interestingly, for a thicker plate (11.23 mm), the data was umbrella shaped. Grady estimates that the sphere broke up into about 440 fragments. In the SPHINX calculations, there were only 1648 particles in the sphere, so calculations with more resolution are needed. These calculations are underway.

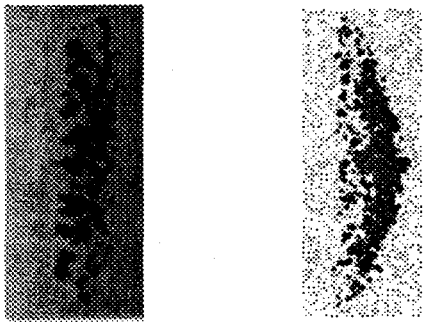

Fig. 3. Experimental data (left) and calculated (right) sphere fragment patterns for the second x-ray position.

Spall in Steel Plates

Mock and Holt (1982) conducted a series of experiments in which they shot a steel flyer plate at a steel target plate. The target was recovered and sectioned so that the pattern of spall cracks is visible. The experiments were conducted at four velocities and for two different steel heat treatments. SPHINX has no model to account for the heat treatment, but experiments for one heat treatment and two velocities were simulated. The SPHINX model for these calculations used the Cagnoux-Glenn damage model with a + 10% random variation in the threshold stress for the start of damage. The Johnson-Cook material strength model was used and a linear Us-Up equation of state. A comparison of the experimental steel plates and the SPHINX results are shown in Figure 4. The crack patterns are in qualitative agreement, but differences in the details exist. These two dimensional cylindrical calculations show that SPHINX has a problem on the symmetry axis.

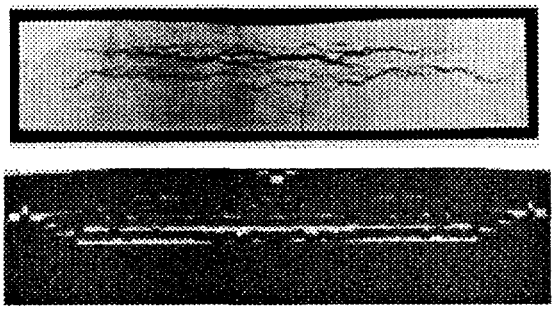

Fig. 4. Experimental data (top) and SPHINX calculations (bottom) for the Mock and Holt steel plate impact experiments.

Tungsten Rod Impacting Heavily Confined Alumina

Several experiments have been done of short tungsten rods impacting heavily confined alumina producing a crack pattern in the alumina (Burkett and Rabern, 1992). We have been simulating this crack pattern using SPHINX and the SPHSFM fracture model. The results of this work are reported in more detail in Mandell, et al., (1996).

The projectile for the experiment was a short, 1.8 cm long and 0.4 cm radius (L/D = 2.25), tungsten rod with a hemispherical nose, a mass of 24 grams, and an initial velocity of 1.288 km/sec. This projectile impacted a target of heavily confined alumina AD85. The alumina was about 9 cm long and 5 cm in radius. Details of the experimental geometry are shown in the left part of Figure 5.

The result from the experiment is shown in the right part of Figure 5. After the impact the target was cut in half, most of the steel confinement removed, and the alumina was dyed so that the features of the data could be easily seen. Because of the slow speed of the projectile, the impact only created a small crater at the top of the alumina. For us, the interesting feature of the data is the crack pattern throughout the alumina, emanating from near the impact point. The goal of the calculations is to reproduce and understand more about these cracks.

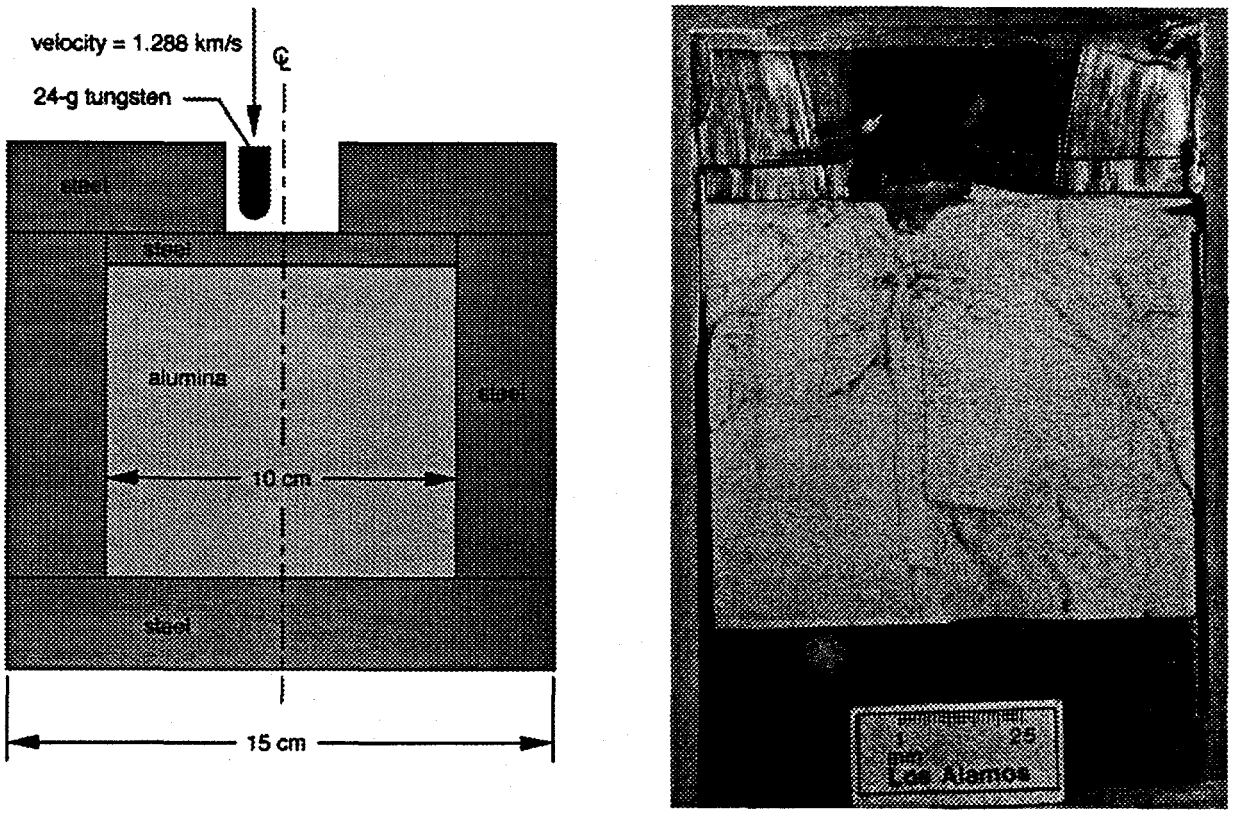

Fig. 5. Experimental setup (left) and experimental data (right) for the alumina impact experiments. The data show a series of cracks in the material.

Calculations of this experiment were done with SPHINX using the SPHSFM model. They were two dimensional plane strain calculations with 55,435 SPH particles and resulted in crack patterns in qualitative agreement with the experiment (Figure 6). A more detailed description of the calculations including parameters that were used can be found in Mandell, et al, (1996). For an equally resolved 3D calculation, about 13 million particles would be required, which would be a very difficult calculation given the current capability of the machines we have. The three-dimensional calculations we made using about 300,000 particles gave poor results. The two-dimensional calculations underpredicted the rod depth of penetration. Two-dimensional calculations with 26,638 particles did not even qualitatively match the experimental crack pattern.

New Directions in Fracture Work

The previous sections discussed the current status of our fracture work. We are now working on creating a new fracture model that differs in a fundamental way from previous models. In the previous models when a particle gets damaged its yield strength is reduced, perhaps to 0., and it becomes a fluid particle but it is still in the calculation. In the new model, we don't damage particles in this manner, rather we break the bonds between the particles. The particles still retain their full material properties, like yield strength; they simply do not interact with particles with a broken bond. Once a bond is broken, a crack and a free surface are created and free surface boundary conditions are applied to the particle. A bond between two particles is broken if the particles are in

tension and if their maximum principle stress exceeds some user-specified value. We feel that this is a more physically realistic model and we hope it will produce better results.

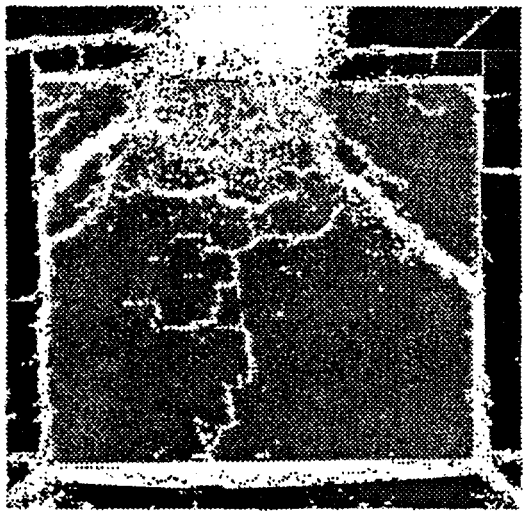

Fig. 6. SPHINX calculation of the alumina impact experiment. This is a 2D, plane strain calculation with 55435 SPH particles. The resulting crack pattern is in qualitative agreement with the data.

Moving Least Squares Interpolation

We have been doing considerable work in the last year trying to improve the SPH method. Most of this work has been done by Gary Dilts. We are at the point of having what appears to be a better SPH method and we are in the process of putting the method in SPHINX so that the method can be adequately explored.

SPH is an interpolation method: fluid quantities at any point, including particle positions, are determined by interpolating from nearby surrounding particles. The interpolating or weight function that we use is a cubic B-spline. Another choice that is sometimes used is a Gaussian function. The basic SPH equation for determining the value of a quantity f at particle location i is

$$f_i = \sum_j^n \frac{m_j}{\rho_j} f_j W_{ij} \tag{22}$$

where m_j, ρ_j and f_j are the nodal values for mass, density and the quantity f. The quantity W_{ij} is the kernel or interpolating function between particles i and j. The sum in this equation runs over all neighbors of particle i. The gradient of a quantity ends up just being sums of gradients of the kernel,

$$\nabla f_i = \sum_j^n \frac{m_j}{\rho_j} f_j \nabla W_{ij} \tag{23}$$

From these simple concepts the equations for SPH fluid dynamics can be derived. Two good reviews detailing the SPH equations have been written by Monaghan (1988) and Benz (1989 and 1990).

While SPH has proven to be a very useful method, particularly in the area of fracture mechanics, it does have problems. The method has an instability that occurs mostly for particles in tension and manifests itself in particle pairing (this is mitigated by using damage). This instability was first pointed out by Jeff Swegle (Swegle, et al., 1995). The interpolation falls off at boundaries which can cause problems in some calculations. SPH uses a particle-particle artificial viscosity which sometimes will produce artificial viscosity when it is not wanted, for example in shear flow.

One approach we are investigating to solving some of these problems is to use a higher order interpolation method. This method is based on the Element Free Galerkin (EFG) method developed by Ted Belytschko (Belytschko, et al., 1994 and Belytschko, et al., 1996). The EFG method uses Moving Least Squares (MLS) interpolants. In this paper, we will only describe the MLS interpolation and discuss the results of a simple test problem. A full description of the MLS method can be found in Dilts (1997).

The basic equation for MLS interpolation is

$$u_i = \sum_j^n \phi_{ij} u_j \tag{24}$$

where u_j are the nodal values and ϕ is the interpolation or weight function given by

$$\phi_{ij} = W_{ij} \boldsymbol{p}_i^T \boldsymbol{A}_i^{-1} \boldsymbol{p}_j . \tag{25}$$

As in SPH, the sum is over the neighbors to particle i. The MLS basis, p, is a polynomial matrix with its transpose given by

$$\boldsymbol{p}_j^T = \{1, x_j, y_j, x_j^2, \ldots\} \tag{26}$$

and $\boldsymbol{A}$ is a matrix given by

$$\boldsymbol{A}_i = \sum_j^n W_{ij} \boldsymbol{p}_j \boldsymbol{p}_j^T . \tag{27}$$

In these equations, W_{ij} is the same weighting function used in standard SPH. The number of elements in $\boldsymbol{p}$ depend on the order of approximation desired and the dimension of the calculation being done. For zeroth order,

$$\boldsymbol{p} = \{1\}, \tag{28}$$

while for first order and three dimensions

$$\boldsymbol{p}_j^T = \{1, x_j, y_j, z_j\} . \tag{29}$$

This interpolation is very similar to SPH, the kernel is just more complicated (much more complicated). In fact, zeroth order MLS reduces to SPH if the zeroth order MLS kernel

$$W_{ij} / \sum_k W_{ik} \tag{30}$$

is replaced by

$$W_{ij} m_j / \rho_j . \tag{31}$$

The point of using the MLS interpolation is that it is better than SPH and still has the nice properties of SPH of being meshless and Lagrangian. Consider for example the Swegle instability test problem - a 1D line of particles in tension and at zero velocity, except for one particle which has a slight velocity perturbation. SPH goes unstable on this problem whereas MLS remains stable for a very long time, although it too starts having slight problems at very late times. MLS does not fall off at boundaries like SPH does. However, MLS is more expensive than SPH.

Stress Difference Method

The stress difference method is similar to standard SPH, but instead of using the sum of the stresses, the stress difference method uses the difference of the stresses. Thus the momentum equation, Eq. 8, using the stress difference method becomes,

$$\frac{d}{dt} U_i^\alpha = \sum_j m_j \left(\frac{\sigma_i^{\alpha\beta}}{\rho_i^2} - \frac{\sigma_j^{\alpha\beta}}{\rho_j^2} \right) \frac{\partial W_{ij}}{\partial x^\beta} . \tag{32}$$

In addition to using the difference between stresses, the stress difference method uses conservative smoothing and renormalization. Like MLS, the stress difference method partially solves the tensile instability problem. Using the stress difference method to solve the tensile instability problem was first proposed by Monaghan and Morris (Monaghan and Morris (1993), Morris (1993)). The method is currently being pursued vigorously by Randles and Libersky (Randles and Libersky (1996)).

Tensile Instability Flyer Plate Example

The following two figures show an example of the tensile instability and solutions for it. The calculation done was a one dimensional aluminum-aluminum flyer plate impact with a flyer plate velocity of 390 meters/second. The details of the calculation are not important for demonstrating the instability. The first figure shows standard SPH results for a stable case, left half, and an unstable case, right half. The top half of the figure for each calculation occurs somewhat after the impact, is in compression and thus is stable. The bottom half of the figure for each calculation is at a later time when the plates are in tension. The calculation in the left half has 1.5 particles per smoothing length and is stable, the calculation on the right half has 1 particle per smoothing length and is unstable. Both the stress difference formulation and MLS eliminate this instability or at least delay it enough so that it is not important. This is shown in Fig. 8 which displays a stress difference calculation on the left and a MLS calculation on the right. These calculations use 1 particle per smoothing length, which is the unstable case for standard SPH, but both the stress difference and MLS results are stable.

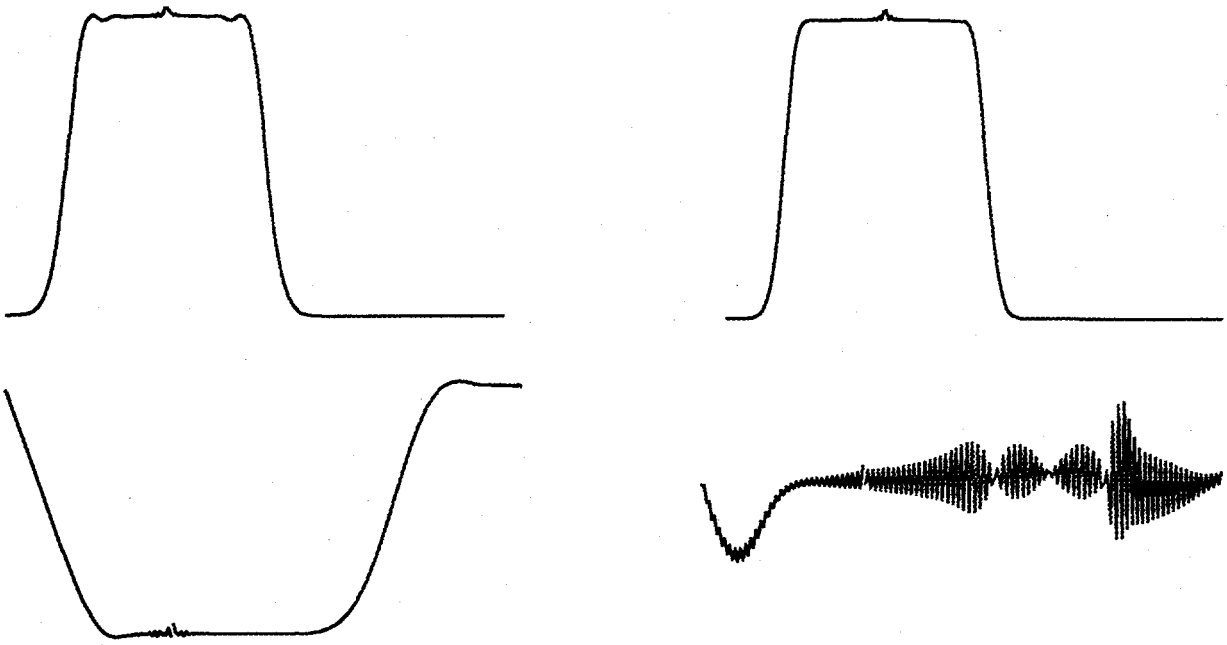

Fig. 7. Results from two standard SPH flyer plate calculations, a stable case on the left and an unstable case on the right. The top half of the figure for each calculation occurs somewhat after the impact, is in compression and thus is stable. The bottom half of the figure for each calculation is at a later time when the plates are in tension.

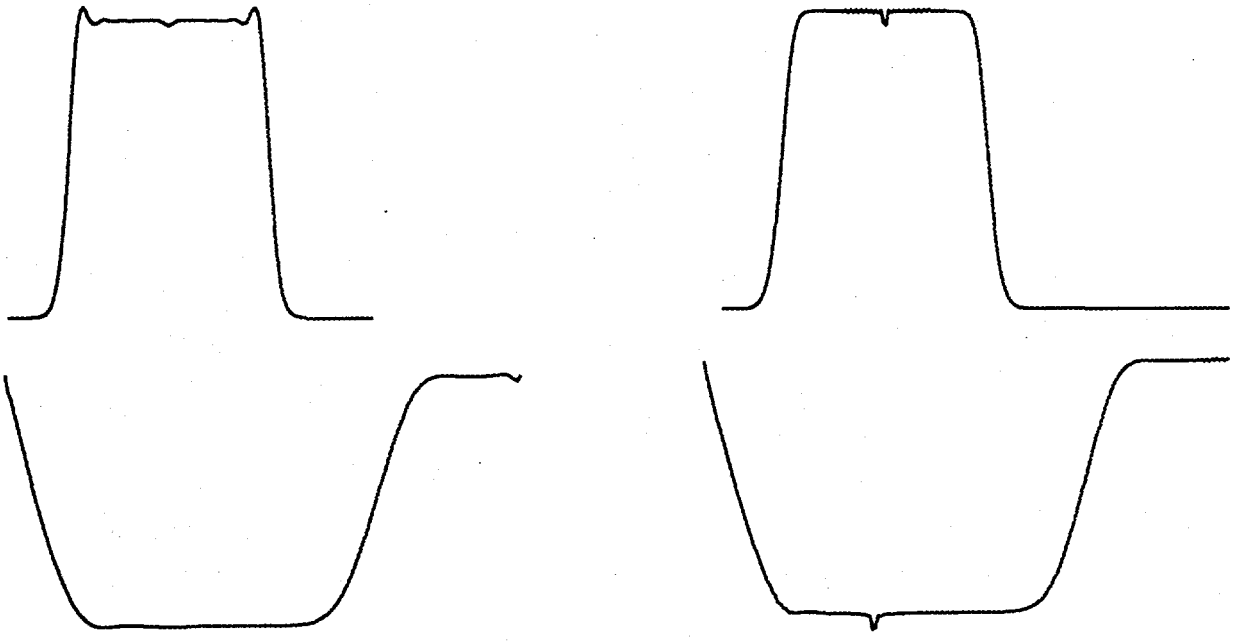

Fig. 8. Results from a SPH stress difference flyer plate calculation, on the left, and an MLS flyer plate calculation on the right. Both calculations are stable.

SUMMARY.

Even with its problems, SPH is a very attractive method and has proven very useful for hypervelocity impacts, particularly those with large void regions. We are attacking the SPH problem areas with the MLS interpolant and the stress difference method. The SPHSFM fracture model is being enhanced to break bonds between particles rather than damage the particles themselves. We continue to work on composites and implicit SPH.

ACKNOWLEDGMENTS.

This research is supported by the Department of Energy and the Department of Defense.

REFERENCES

Ashby, M. F. and Jones, D. R. H., Engineering Materials 2, Pergamon Press, New York, (1988).

Belytschko, T., Lu, Y. Y., and Gu, L., "Element-Free Galerkin Methods" Int. J. for Numerical Methods in Engineering, **37**, 229-256 (1994).

Belytschko, T., Kronaguz, Y., Organ, D., Fleming, M., Krysl, P., "Meshless Methods: An Overview and Recent Developments", preprint (1996).

Benz, W. Smooth Particle Hydrodynamics: A Review, Harvard-Smithsonian Center for Astrophysics Preprint No. 2884 (1989).

Benz, W., "Smooth Particle Hydrodynamics: A Review," The Numerical Modeling of Nonlinear Stellar Pulsations, (J. R. Buchler (ed.), 1990) pp. 269-288.

Benz, W. and Asphaug, E., "Impact Simulation with Fracture: I. Methods and Tests," ICARUS, **107**, 98-116 (1994).

Benz, W. and Asphaug, E., "Simulations of Brittle Solids Using Smooth Particle Hydrodynamics," Computer Physics Communications, **87**, 253-265 (1995).

Burkett, M. W. and Rabern, D. A., "Stress Fields Generated by Kinetic Energy Projectile Interaction With Ceramic Targets," Shock Compression of Condensed Matter, ed. by S. C. Schmidt, R. D. Dick, J. W. Forbes, and D. G. Tasker, 947-950, Elsevier Science Publishers (1992).

Cagnoux, J., "Modele Phenomenlogique D'Ecaillage D'Un Pyrex" (Phenomenological Model of Spalling of Pyrex Glass), Journal De Physique, Colloque C5, supplement au n o 8 Tome 46, (1985).

Crow, E. L., Davis, F. A. and Maxfield, M. W., Statistics Manual, Dover Publications, Inc., New York, (1960).

Dilts, G. A. Moving-Least-Squares-Particle Hydrodynamics I, Consistency and Stability. Los Alamos Report LA-UR-97-4168 (1997). This paper is also available on the world wide web as a PostScript file at http://www-xdiv.lanl.gov/XHM/SPH/papers/mls/mlsphI.ps.

Gingold, R. A. and J. J. Monaghan. Smoothed Particle Hydrodynamics: Theory And Application To Non Spherical Stars, Mon. Not. Roy. Astron. Soc. **181**, 375-389 (1977).

Gingold R. A. and J. J. Monaghan. Kernel Estimates as a Basis for General Particle Methods in Hydrodynamics, J. Comput. Phys. **46**, 429-453 (1982).

Glenn, L. A., Moran, B. and Kusubov, A., "Modeling Jet Penetration In Glass," Conference on the Application of 3-D Hydrocodes to Armor/Anti-Armor Problems, Ballistic Research Laboratory, Aberdeen Proving Grounds, MD, (1990).

Grady, D. E. and Kipp, M. E., "Experimental Measurement of Dynamic Failure and Fragmentation Properties of Metals," Int. J. Solids Structures, **32**, 2779-2791 (1995).

Henninger, R. J., Mandell, D. A., Huyett, R. A. and Lyons, F. S., "Improvement of Glass-Plastic Transparent Armor Using Computational Modeling," Sixth Annual US TARDEC Combat Vehicle Survivability Symposium, Monterey, CA (1995).

Libersky L. D., and A. G. Petschek. Smooth Particle Hydrodynamics with Strength of Materials, *Advances in the Free-Lagrange Method,* (Trease, Fritts, and Crowley, eds.), Springer Verlag, 248 (1990).

Lucy, L. A Numerical Approach To Testing the Fission Hypothesis, Astron. J., 82, 1013-1024 (1977).

Mandell, D. A. and Wingate, C. A., "Numerical Simulations of Glass Impacts Using Smooth Particle Hydrodynamics," 1995 APS Topical Conference on Shock Compression of Condensed Matter, Seattle, WA (1995).

Mandell, D. A., Wingate, C. A. and Stellingwerf, R. F., "Prediction of Material Strength and Fracture of Brittle Materials Using the SPHINX Smooth Particle Hydrodynamics Code," Proceedings of the 10th ASCE Engineering Mechanics Conference, Boulder, CO, (1995).

Mandell, D. A., Wingate, C. A. and Schwalbe, L. A., "Simulation of a Ceramic Impact Experiment Using the SPHINX Smooth Particle Hydrodynamics Code," Proceedings of the 16th International Ballistic Symposium, San Francisco, CA, September 23-27, 1996. This paper is available on the World Wide Web at the following address: http://www-xdiv. lanl.gov/XHM/SPH/papers/Ballistic/16th_Ballistic_Symposium.pdf

Mock, Willis Jr. and Holt, William H., "Determination of Dynamic Fracture Parameters for HF-1 Steel," J. Appl. Phys., **53**, 5660-5668 (1982).

Monaghan, J. J. Why Particle Methods Work, SIAM J. Sci. Stat. Comput. **3**, 422-433 (1982)

Monaghan, J. J. Particle Methods for Hydrodynamics, Comp. Phy. Rep. **3**, 71-124 (1985).

Monaghan, J. J. An Introduction to SPH, Comput. Phys. Comm. **48**, 89-96 (1988).

Monaghan, J. J. and Morris, J. A. SPH Masters Negative Stress. Workshop on Advances in Smooth Particle Hydrodynamics, Los Alamos Report LA-UR-93-4375, pages 11-27, (1993)

Morris, Joseph Peter Anthony. A Study of the Stability Properties of SPH. preprint (1993).

Randles, P. W., Carney, T. C. and Libersky, L. D., "Continuum Dynamical Simulations of Bomb Fragmentation," Proceeding of the 15th International Symposium on Ballistics, Jerusalem, Israel, May 21-24, 1995.

Randles, P. W. and Libersky, L. D., "Smoothed Particle Hydrodynamics: Some Recent Improvements and Applications," Computer Methods in Applied Mechanics and Engineering (in press, 1996).

Schonberg, W. P., R. A. Taylor, and J. R. Horn. An Analysis of Penetration and Ricochet Phenomena in Oblique Hypervelocity Impact, NASA TM-100319 (1988).

Stellingwerf, R. The SPH_C Manual, User's Guide, Programmer's Guide, Technical Guide, Function Reference, Test Cases, Mission Research Corporation report AMRC-N-384.1-384.5 (1989a)

Stellingwerf, R. F. Boundary Condition Tests Using Smooth Particle Hydrodynamics, Mission Research Corporation report MRC/ABQ-N-426 (1989b).

Stellingwerf, R. F. Blast Wave Stability in Nuclear Explosions I, Mission Research Corporation report MRC/ABQ-R-1254 (1990a).

Stellingwerf, R. F. Smooth Particle Hydrodynamics, *Advances in the Free-Lagrange Method,* (Trease, Fritts, and Crowley, eds.), Springer Verlag, 239 (1990b).

Stellingwerf, R. F. and R. E. Peterkin. Smooth Particle Magnetohydrodynamics, Mission Research Corporation report MRC/ABQ-R-1248 (1990).

Stellingwerf, R. F. Shock Tests for Smooth Particle Hydrodynamics, LANL memo X-1(1/92)29 (1992).

Stellingwerf, R. F. and Schwalbe, L. A., "Statistical Fracture Models For Smooth Particle Hydrodynamics," Los Alamos Memorandum X-1(1/95)-9 (1995).

Swegle, J. W., Hicks, D. L. and Attaway, S. W., "Smoothed Particle Hydrodynamics Stability Analysis," J. Comput. Phys., **116**, 123-134, (1995).

Weibull, W., "A Statistical Distribution Function of Wide Applicability", J. Appl. Mech. **18**, 293-297, (1952).

Wingate, C. A. and H. N. Fisher. Strength Modeling in SPHC. Los Alamos Report, LA-UR-93-3942 (1992).